La mer 32: 19–30, 1994
Société franco-japonaise d'océanographie, Tokyo

Use of pH to trace water masses in the Weddell Sea*

Chen-Tung Arthur CHEN**

Abstract: When plotting the pH data obtained in the eastern Weddell Sea vs. potential temperature (θ), a distinct break exists in the slope near $\theta = 0.08°C$ and $\sigma_4 = 46.06$. A less pronounced break in slope occurs at $\theta = -0.6°C$ and $\sigma_4 = 46.16$. Total CO_2, pCO_2 and silicate data also show similar discontinuities. The breaks in the pH slopes probably result from, and can be used to help identifying the lateral spreading of deep- and bottom-water masses.

1. Introduction

Deep waters from the three oceans move to the Southern Ocean. The resultant relatively homogeneous water (MONTGOMERY, 1958; CARMACK, 1977) becomes the major source of the Antarctic Bottom Water (AABW), which spreads back into the deep world oceans (WUST, 1939; LYNN and REID, 1968). The Weddell Sea is considered the major source of the AABW (DEACON, 1937; REID and LYNN, 1971; CARMACK and FOSTER, 1975; CARMACK, 1990).

Relative homogeneity of the water masses, however, results in small signals for traditional tracers such as θ, S, and oxygen. As a result, it is more difficult to clearly identify the end members of the water masses.

On the other hand, it is not unexpected that the deep Weddell Sea waters possess distinct regimes despite of the relative homogeneity (CALLAHAN, 1972; REID *et al*, 1977; SCHLEMMER, 1978; FOSTER and MIDDLETON, 1979; GORDON, 1978, 1982; CHEN and RODMAN, 1985, 1990; ORSI, *et al.*, 1993). In this report I will use pH, total CO_2, pCO_2 and silicate data in addition to the traditional tools to identify in more detail the water-mass characteristics of the important end-members. These end members constitute the water masses in the Weddell Sea either directly or indirectly. Data were mainly collected on the Soviet icebreaker SOMOV during the US-USSR Weddell Polynya Expedition in the late austral winter and early spring of 1981 (HUBER *et al.*, 1983; CHEN, 1984). Additional GEOSECS, AJAX and Polarstern data (GEOSECS, 1981; CHIPMAN *et al.*, 1986; CHIPMAN and TAKAHASHI, 1990) are also used.

* Received January 30, 1994
** Institute of Marine Geology, National Sun Yat-Sen University, Kaohsiung, Taiwan, R. O. C.

2. pH, total CO_2, pCO_2, and silicate signals

The study area and the cruise track are shown in Fig. 1. The pH samples were all determined at $25 \pm 0.02°C$ with a combination electrode within 30 minutes. NBS 4.004 and 7.415 buffers were used to calibrate the electrode. In addition, a NBS 6.863 buffer plus three buffers 4.01, 6.86 and 9.18 prepared by V. FEDOROV (the Arctic and Antarctic Research Institute of the USSR) were measured. The results agreed with the prepared values to 0.005 ± 0.005. The reproducibility of the pH measurements was better than ± 0.003 units for 4 replicates of each sample. The electrode drift was determined approximately every two weeks. The largest drift was found to be 0.001 unit/day and the correction was made to the measured values (CHEN, 1984).

Alkalinity was determined at $25 \pm 0.02°C$ with a Radiometer TTT61 Digital Titrator with a reproducibility of better than ± 4 μmol/kg for replicate samples. Some samples were also measured using the method of CULBERSON *et al.* (1970) with similar precision. No systematic difference was found between these two sets of data. All samples were stored in amber plastic bottles, and the alkalinity measurements were accomplished within 12 hours after samples were aboard. Total CO_2 (TCO_2) and pCO_2 were calculated from pH and alkalinity with a precision of 5 μmol/kg and 5 μatm, respectively. In Fig. 2 is plotted potential temperature (θ) vs. pH for the deep SOMOV data (CHEN, 1984).

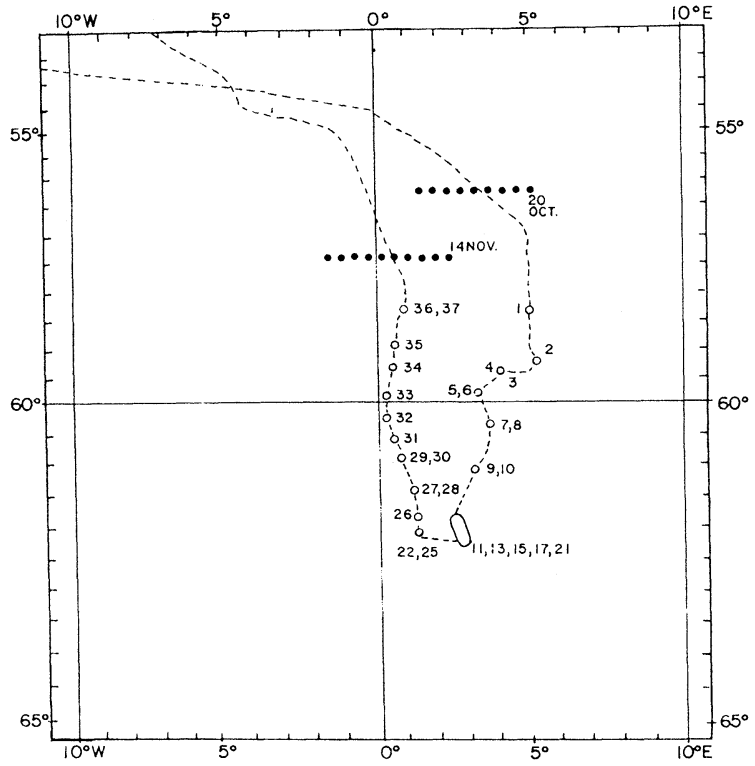

Fig. 1. Location of the SOMOV vertical stations. Dotted lines at 20 Oct. and 14 Nov. 1981 locate the ice edge.

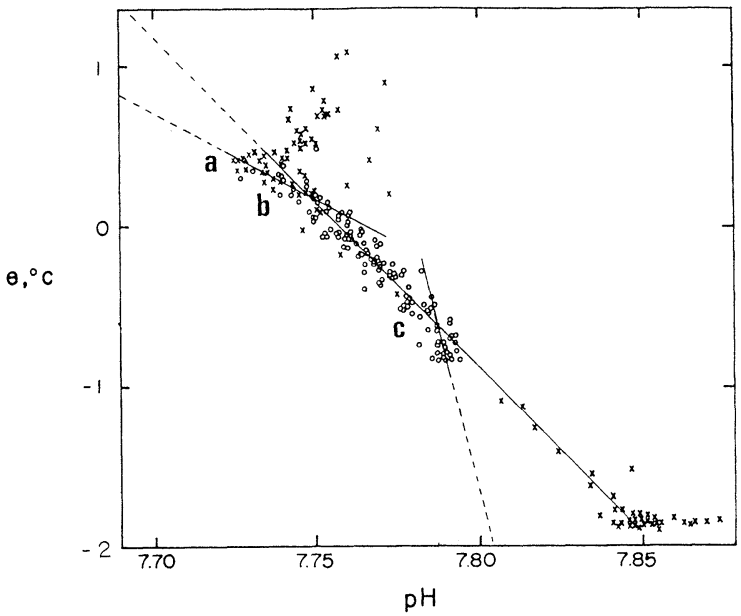

Fig. 2. Composite SOMOV potential temperature vs. pH diagram for data below the salinity maximum; x's are data above salinity maximum. Characteristics of a, b and c are listed in Table 1 and discussed in the text.

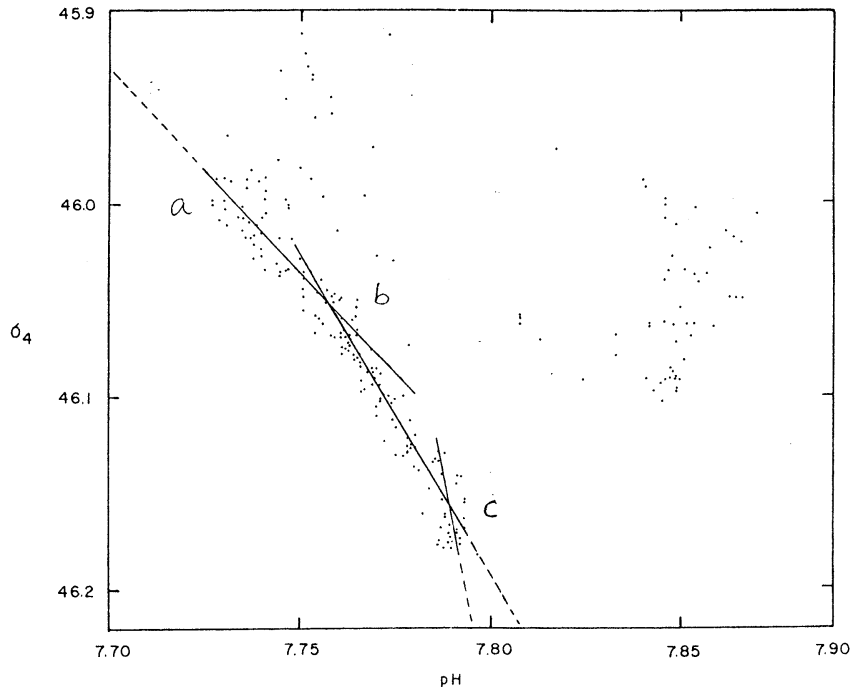

Fig. 3. Composite SOMOV sigma-4 vs. pH diagram. Characteristics of a, b and c are listed in Table 1 and discussed in the text.

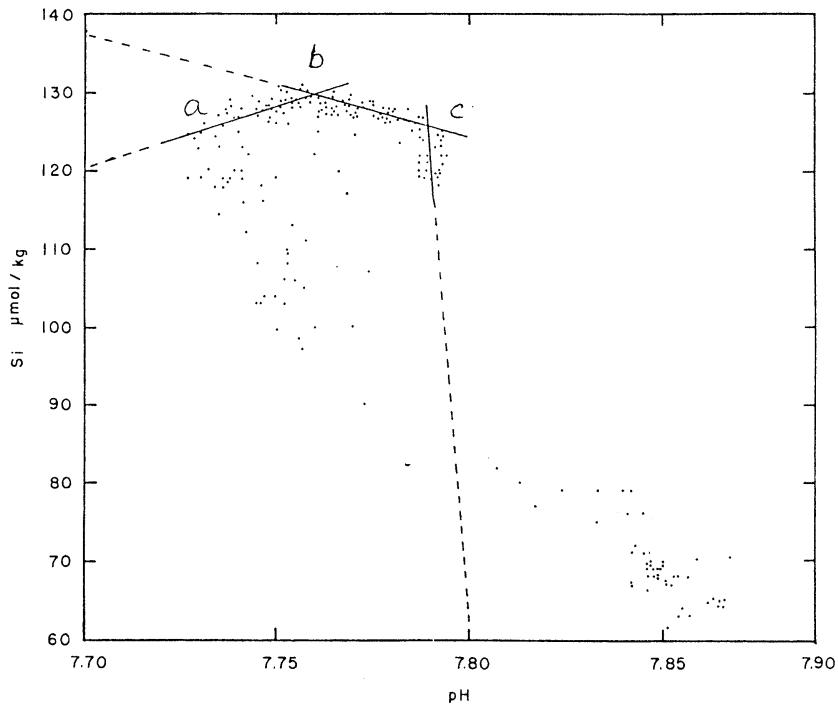

Fig. 4. Composite SOMOV silicate vs. pH diagram. Characteristics of a, b and c are listed in Table 1 and discussed in the text.

Table 1. Characteristics at the Deep-Water Discontinuities in the Weddell Sea

	TOP-(a)[1]	BREAK 1-(b)[1]	BREAK 2-(c)[1]
T (°C)[2]	0.19−0.2°C	0.05 to 0.08	−0.5 to −0.6
pH	7.73	7.750 to 7.757	7.779 to 7.789
TCO_2 (μmol/kg)	2282	2280	2268
pCO_2 (μatm)	520	510	460
S	34.680	34.683	34.660
Si (μmol/kg)	124.5	129.5	125.5
AOU (μmol/kg)	148	135	111
σ_θ	27.828	27.843	27.861
σ_2	37.123	37.158	37.219
σ_4	46.00	46.056	46.156
Av. depth (m)	312 ± 151	1241 ± 131	3944 ± 156

(1) TOP refers to the top of the deep water, see Fig 2. for locations of a, b, c

(2) The ranges recorded are due to slightly different values given when different parameters are plotted.

There is a distinct break in slope near $\theta = 0.08$ °C and a less pronounced break near $\theta = -0.5 \sim -0.6$°C. When σ_4 (Fig. 3; density reference to 4000dB surface, REID and LYNN, 1971) is plotted against pH, changes in the pH slope are seen at $\sigma_4 = 46.06$ and 46.16. The $\sigma_4 = 46.06$ layer separates the circumpolar water and the Weddell Sea Deep Water (WSDW) whereas the $\sigma_4 = 46.016$ layer separates WSDW from the Weddell Sea Bottom Water (WSBW, ORSI *et al.*, 1993).

The deeper discontinuity, at $\sigma_4 = 46.16$, is more distinctly shown in the silicate/pH diagram (Fig. 4), than on the other figures. Table 1 gives the characteristics of the two discontinuities determined from the complete SOMOV data set. The depth, the σ_2 (density reference to 2000dB surface) and the σ_θ surface associated with the appropriate σ_4 surface are average values computed from the total SOMOV data. AOU is the apparent oxygen utilization which is the difference between the measured oxygen concentrations and the saturated values calculated using CHEN (1981).

TCO_2 of the Weddell seawater seems to mix conservatively below the S_{max} layer. The normalized TCO_2 ($NTCO_2 = TCO_2 \times 35/S$) values calculated from pH and alkalinity data for all SOMOV stations below the S_{max} layer are plotted vs. θ in Fig. 5. A linear correlation is observed with a standard deviation of 6 μmol/kg.

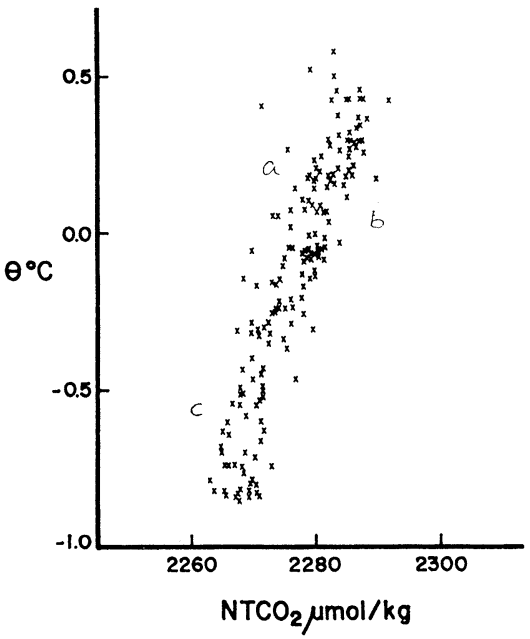

Fig. 5. θ / $NTCO_2$ correlation below the maximum salinity layer. Characteristics of a, b and c are listed in the Table 1 and discussed in the text.

Since the standard deviation of the least-squares fit is only slightly larger than our analytical precision of ± 5 μ mol/ kg, station-to-station variation is minimal. The change in slope at approximately −0.6° C is not apparent. No break in slope near 0.1° C is observed.

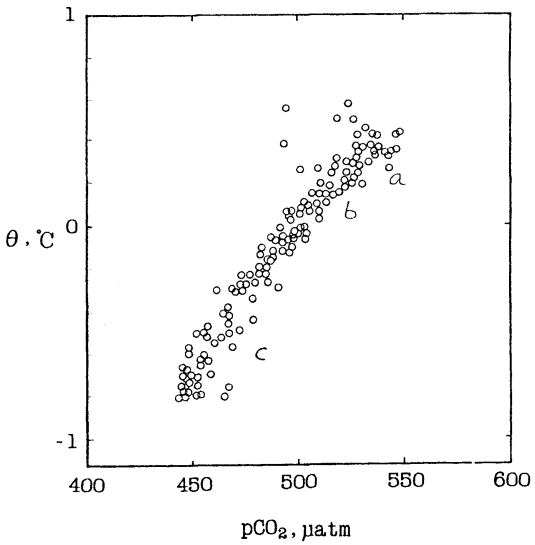

Fig. 6. θ /pCO_2 correlation for all SOMOV samples below the maximum salinity layer.

The calculated pCO_2 values correlate with θ (Fig. 6) in a way similar to the correlation between $NTCO_2$ and θ. There is a pCO_2 maximum near the S_{max} layer. Below it the pCO_2 decreases roughly linearly with decreasing temperature, but a steeper slope is observed below approximately $-0.6°$ C. The shallower break is also not as apparent. The pCO_2 data of the AJAX and Polarstern expeditions (CHIPMAN *et al.*, 1986; CHIPMAN and TAKAHASHI, 1990) show the same trends.

3. Discussion

The structure seen on the property diagrams is not apparent in the vertical section of z/pH (Fig. 7) and the reason for the breaks in slopes on Figures 2 to 4 is not obvious from the vertical distribution of pH. However, that the deep waters possess distinct regimes (3 from the pH analysis) is not unexpected. In the Southwestern Atlantic, REID *et al.* (1977) have shown that stability maxima associated with different density surfaces exist in the deep and bottom waters. They pointed out that the stability maxima should be boundaries between core layers and that these maxima are maintained over long distances by lateral processes. SCHLEMMER (1978) has made an extensive study of bottom waters in the Antarctic ocean and investigated the distribution of properties on six σ_4 surfaces which marked the boundaries of various abyssal water masses and/or were characterized by changes in gradients. GORDON (1982) has made a detailed study of WSDW variability, FOSTER and MIDDLETON (1979) and ORSI *et al.*, (1993) analyzed the variability within the bottom water of the Weddell Sea. We believe that the pH slope breaks result from similar lateral spreading of deep and bottom water masses.

In Table 2 the water-mass characteristics have been presented for the important end-members which should affect this region either directly or indirectly. It should be noted that the values given for the Circumpolar Deep Water (CDW) components represent a concentrated mass in the Southwestern Atlantic. Also the WSDW may have a relatively large non-steady state temperature and salinity range (GORDON, 1982).

Significant dilution of these deep water end-members has occurred in transit to the basins near Antarctica, probably with a complex mixing history (CALLAHAN, 1972). The CDW entering the Southwestern Atlantic has low oxygen and high nutrients which originate from the Pacific Deep Water, PDW. It encounters in the same density range the higher oxygen, lower nutrient and markedly higher salinity North Atlantic Deep Water (NADW) (REID *et al.*, 1977). The incorporation of the NADW into the CDW results in a low-oxygen component above a broader high-salinity component which becomes decreasingly separated vertically upon approaching the Antarctic Continent (see for example plates 110, 111, 113 in GORDON *et al.*, 1982). The CDW undergoes further modification in the Weddell Sea by the input of Antarctic components, becoming considerably colder, fresher, more oxygenated, and starting to show traces of anthropogenic components such as tritium, carbon 14, freons, and fossil fuel CO_2 (WEISS *et al*, 1979; CHEN, 1982; POISSON and CHEN, 1987; CHEN and RODMAN, 1990; ANDERSON *et al.*, 1991). The CDW is now essentially a new deep water mass frequently referred to as WSDW (GORDON, 1978; GORDON and H UBER, 1984); however, the low oxygen signal overlying a high salinity signal is still

Table 2. Water Mass Characteristics in the Drake Passage, South Atlantic and Weddell Sea

	θ (°C)	S	O_2(ml/l)	SiO_2(μmol/kg)
Winter Surface Water (WW)	t_f to −1.5[1]	33.8 to 34.6[1][2]	6.9 to 7.5[3a]	70[3a]
Summer Surface Water (SW)	$>t_f$[1]	<34.2[2]	>7.8[3]	70[2]
Shelf Water	t_f to −1.5[1]	34.2 to 34.8[1]	7.1[3d]	70[3d]
Modified Warm Deep Water[6]	−1.6 to 2[1]	34.35 to 34.7[1]	5.5 to 7.2[2]	65 to 85[2]
Weddell Sea Deep Water (WSDW)[6]	0 to 2[1]	34.65 to 34.75[1]	4.3 to 5.3[3]	90 to 120[3]
Pacific Deep Water (PDW)	1.8 to 2.5[4][5c]	34.55 to 34.7[4][5c]	3.7 to 4.6[4][5c]	60 to 100[4][5c]
North Atlantic Deep Water (NADW)	2 to 3[4][5d]	34.8 to 34.95[4][5d]	4.5 to 5.5[4][5d]	50 to 70[4][5d]
Weddell Sea Bottom Water (WSBW)	<−.7[7]	34.65[7]	6.5[7]	95 to 115[8]
Antarctic Bottom Water (AABW)	−0.4° to 0°[7][8]	34.6 to 34.68[7][8]	5.4 to 5.8[7][8]	110 to 125[8]

(1) CARMACK, (1977); the t_f refers to freezing temperature
(2) CARMACK, (1974)
(3) WEISS *et al.* (1979)
  (a) These values have been taken from the temperature-minimum water
  (b) Summer values
(4) GEOSECS Atlantic Expedition Vol. 2 (1981): plates 3, 5, 11, 15 are the Western Atlantic and into the Scotia Sea; plates 55 and 59 are for the Drake Passage; oxygen values are given in μM/kg and have been converted to ml/l.
(5) GORDON *et al.* (1982)
  (c) plates 184, 185, 186 are a detailed transect across the Drake Passage.
  (d) plate 104 is for the South Atlantic
(6) Weddell Sea Deep Water is also sometimes referred to as warm deep water.
(7) FOSTER and MIDDLETON (1979)
(8) CARMACK (1973)
(9) The upper boundary of AABW has been somewhat arbitrarily chosen to be 0° to fit with the lower boundary of WSDW.

identifiable. Within the shelf domain the WSDW is further modified.

End-members were estimated from Table 2 and from Figs. 2–6. Because precise pH measurements are non-existent for most of these water masses, assigning end-member points in these figures is somewhat tentative. In looking for the end-member (Fig. 2) for the regime denser than σ_4=46.156 (Fig. 3), we note that a shelf component at freezing temperature would have a pH of about 7.80 to 7.81. This translates from extrapolation on Figure 8 into a salinity range of 34.65 to 34.66, easily within the shelf-water range in view of the large salinity spread it may have (Table 2). However, shelf-water components in bottom-water formation must be of these higher salinity varieties.

For the warmer end-member, the WSDW end of this mixing line defined at a temperature of 0.8−1.2° C, we see a pH of about 7.76 and, thus,

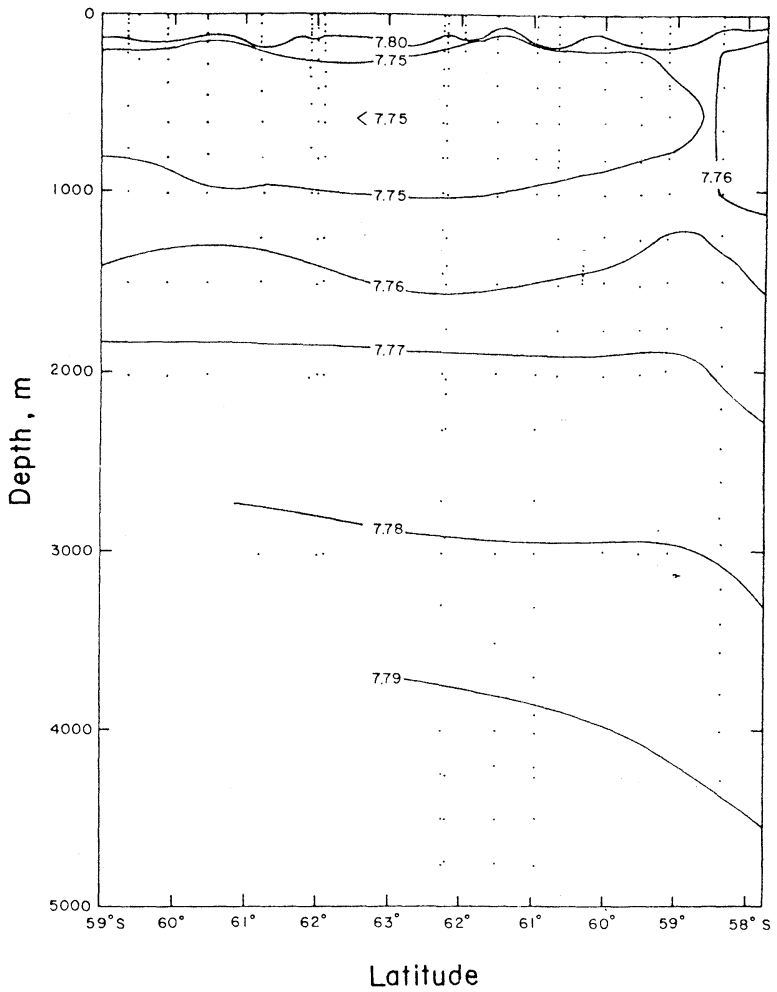

Fig. 7. Cross-section of the SOMOV pH data (at 25°C).

again by extrapolation on Figure 8, a salinity of 34.66 to 34.67. These salinities correspond to the range of WSDW (Table 2). When this mixing line is extended to 2.5 to 3°C the corresponding pH of 7.73–7.74 gives a salinity of at most 34.69, much below that for NADW. However, from the combined SOMOV θ/S data (Fig. 8, GORDON and HUBER, 1984) we can see that the abyssal regime has a non-isopycnal scatter which would also give significantly lower salinities than NADW from a simple two component mixing line, indicating a complex mixing history for the predominantly isopycnally spreading deep waters. Extension of the mixing line for the second regime (σ_4=46.056 to 46.156) to the warmer end-member WSDW component at 0.8−1°C gives a pH of 7.71−7.72 and a corresponding extrapolated salinity of 34.70 to 34.71. Further extension of the line to 2.5° −3°C gives a pH of 7.60−7.64 and a salinity extrapolated to 34.79 to 34.83, consistent with values for NADW (Table 2). The cold end-member for this mixture can be explained as Winter Water (WW) at freezing, with a pH of 7.85 and thus an extrapolated salinity of 34.60.

The upper regime between a σ_4 of 45.900 and 46.056 can be explained as a mixture of WW (t_f =freezing temperature, pH=7.92 — 7.94, S=34.67 to 34.68) and the oxygen-poor component of WSDW. For example, at t=0.6 to 0.8 °C the pH is 7.69 to 7.71 which then gives a salinity of 34.68 to 34.69. Extending this mixing

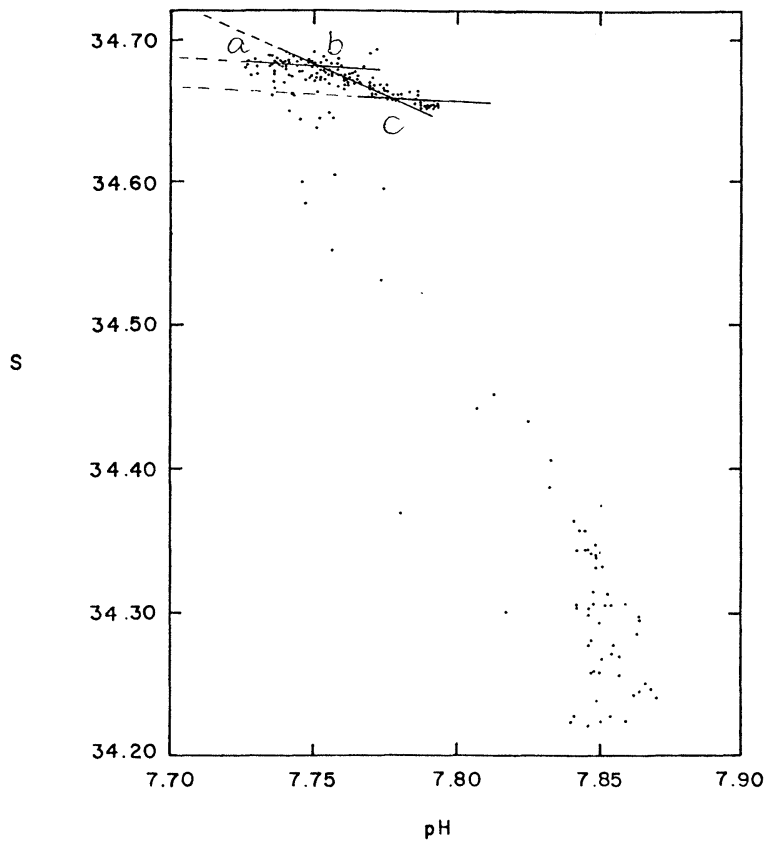

Fig. 8. Composite SOMOV salinity vs. pH diagram. Characteristics of a, b and c are listed in Table 1 and discussed in the text.

line to even warmer values of 2−2.5° C of PDW will give extrapolated salinities in the range 34.68 to 34.70 from a pH range of 7.54 to 7.59.

Vertical convection of WW with entrainment of WSDW at progressively more southern locations, or deeper convection by increasingly dense WW, or a combination of these two effects, and subsequent spreading of the mixture after reaching their equilibrium density, may explain these separate deep water regimes. The bottom-water regime is similarly explained, but instead of winter water entering directly into the mixing processes, shelf water is entraining modified deep water. Observed variability in the WSBW, (Table 2), a subclass of AABW on a year's time scale, may in part be related to seasonal effects (FOSTER and MIDDLETON, 1979). It is significant to this study that CARMACK and FOSTER (1975) note a θ/S discontinuity near -0.5° C and $\sigma_4 = 46.175$ which they attribute to either older re-circulated WSBW or an additional AABW component. KRYSELL (1992) plotted carbon tetrachloride and methyl chloroform concentrations vs θ and also found a distinct break at -0.5° C. The man-made chemicals could only be detected in the cold bottom waters with $\theta < -0.5$° C. This water is the most ventilated of all subsurface waters with the highest oxygen, tritium and C−14 (Table 2; CHEN and RODMAN, 1990). CHEN and RODMAN (1990) also reported that bottom waters denser than $\sigma_4 = 46.156$ contain some anthropogenic CO_2.

Shelf-water modified deep water mixtures and subsequent spreading at depths have been analyzed off Wilkes Land by CARMACK and KILWORTH (1978) and observed off Enderby Land (JACOBS and GEORGI, 1977). In both cases they observed plumes formed. But the data here suggest a broader spatial effect, since the three

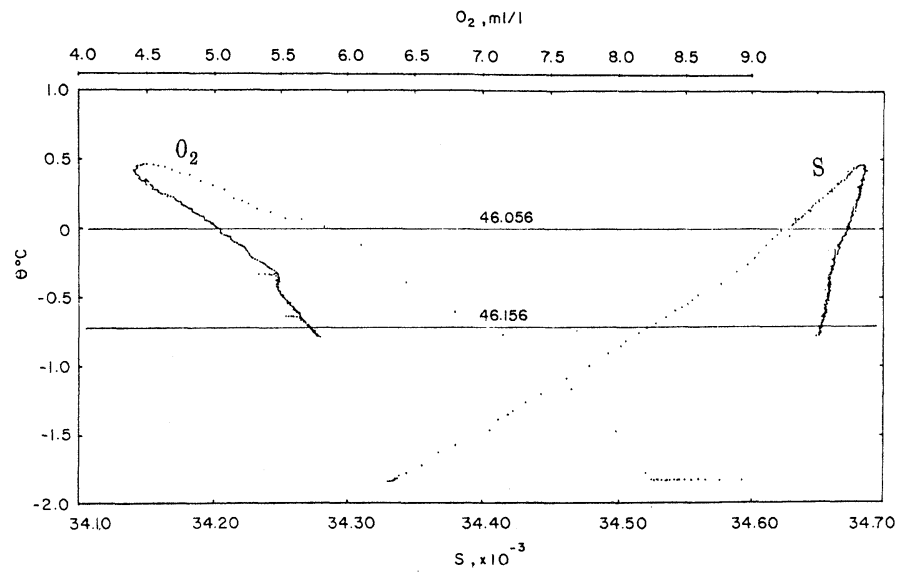

Fig. 9. SOMOV station 30 oxygen and potential temperature vs. salinity taken from the oxygen probe and CTD. The σ_4 surfaces which encompass the two breaks (Table 1) are shown (taken from HUBER *et al.*, 1983).

regimes extend over several kilometers depth and well north of the Antarctic continent. The cyclonic circulation (KLEPIKOV, 1960; DEACON, 1976, 1979; CARMACK and FOSTER, 1975) in the Weddell Sea may enhance and spread the effect of plume injection by providing a longer path for alterations to occur. Major injection of surface water directly into the deep-water regime via deep convection has been observed in this region (GORDON, 1978), and modeling studies (KILWORTH, 1979; MARTINSON *et al.*, 1981) have shown that large areas of the Weddell Sea may be subject to this deep convection, called chimneys. GORDON (1982) hypothesizes that chimney convection results in the significant temporal and spatial thermal alterations (the θ_{max} is lowered by as much as 0.4° C) observed between 250 m and 2700 m over broad areas. It is interesting to note that anomalously oxygenated fresh water is observed well north of the Antarctic continent in the deep water between σ_4 of 46.056 and 46.156. (Fig. 9).

Figure 10 shows a potential density section of pH data for the eastern stations of the SOMOV track. The mixed layer is at densities less than a σ_θ of about 27.65, and the pycnocline extends to a σ_θ of about 27.80. Few data points exist in the pycnocline so the contour interval is necessarily coarser and more subjective. Below $\sigma_\theta = 27.8$ the isopleths of pH become increasingly level showing that the distribution of pH is dominated by isopycnal spreading. Some structure is seen in the 7.750 and 7.740 pH contours where they bow slightly upward at stations 7 and 9 indicating some non-isopycnal spreading. The density surfaces less than a σ_θ of 27.82 curve slightly downward at these stations (see Fig. 2 in GORDON and HUBER, 1984), and thus the pH contours lying more horizontally with respect to density contours (shown by GORDON and HUBER, 1984) would account for the observed bowing of the pH isopleths. The minimum pH lies from a σ_θ of 27.82 to 27.84 which is the density range containing the oxygen minimum. Thus the spread of pH in the deep and bottom waters is very much isopycnal.

4. Conclusion

pH is easy to measure, has high precision and accuracy, and the analysis for 12 Rosette samples (4 replicates for each sample) can be done within 30 minutes (CHEN, 1984; BYRNE *et al.*, 1988). It proves to be very useful in studying water masses in the Weddell Sea. Distinctive breaks in the pH vs θ plots at $\theta = 0.08$° C and -0.6° C were related to spreading of deep- and

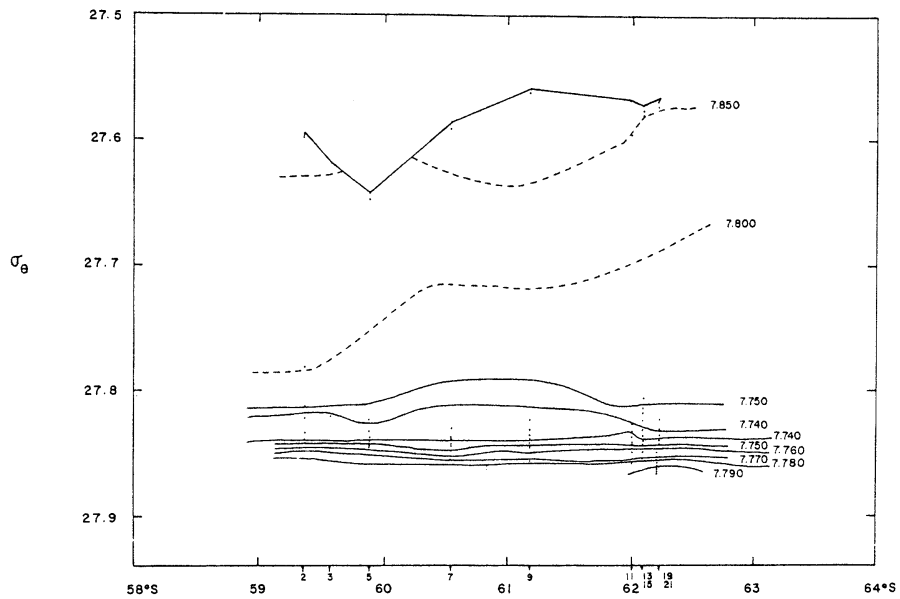

Fig. 10. SOMOV section of pH for stations along the eastern track (see Fig. 1) with potential density as the ordinate. Note the change in contour interval for densities less than $\sigma_\theta = 27.80$.

bottom-water masses in the Weddell Sea.

Acknowledgements

I acknowledge the financial support of the National Science Council (NSC 83-0209-M110-002K). M. RODMAN provided valuable comments.

Refferences

ANDERSON, L. G., O. HOLBY, R. LINDEGREN and M. OHLSON (1991): The transport of anthropogenic carbon dioxide into the Weddell Sea. J. Geophys. Res. **96**, 16679-16687.

BYRNE, R. H., G. ROBERT-BALDO, S. W. THOMPSON and C. T. CHEN (1988): Seawater pH measurements: an at-sea comparison of spectrophotometric and potentiometric methods. Deep-Sea Res. **35**, (8), 1405-1410.

CALLAHAN, J. E. (1972): The structure and circulation of Deep Water in the Antarctic. Deep-Sea Res. **19**, 563-575.

CARMACK, E. C. (1973): Silicate and potential temperature in the deep and bottom waters of the western Weddell Sea. Deep-Sea Res. **20**, 927 932.

CARMACK, E. C. (1974): A quantitative characterization of water masses in the Weddell Sea during summer. Deep-Sea Res. **21**, 431-443.

CARMACK, E. C. (1977): Water characteristics of the Southern Ocean south of the Polar Front. *In*: A Voyage of Discovery, George DEACON 70th Anniversary Volume, M. ANGEL (ed.), Pergamon Press, Oxford, 15-41.

CARMACK, E. C. (1990): Large-scale physical oceanography of polar oceans. Polar Oceanography, Part A. : Physical Science, 171-222.

CARMACK, E. C. and T. D. FOSTER (1975): On the flow of water out of the Weddell Sea. Deep-Sea Res. **22**, 711-724.

CARMACK, E. C. and P. D. KILWORTH (1978): Formation and interleaving of abyssal water masses off Wilkes Land, Antarctica. Deep-Sea Res. **25**, 357-359.

CHEN, C. T. (1981): Oxygen solubility in seawater. *In*:Solubility Data Series V. 7, Oxygen and Ozone, R. BATTINO (ed.), Pergamon Press, 41-55.

CHEN, C. T. (1982): On the distribution of anthropogenic CO_2 in the Alantic and Southern Oceans. Deep-Sea Res. **29**, 563-580.

CHEN, C. T. A. (1984): Carbonate chemistry of the Weddell Sea, U.S. DOE Tech. Rep. DOE/EV/10611-4, 118pp.

CHEN, C. T. (1988): Summer-winter comparisons of oxygen, nutrients and carbonates in the polar seas. La mer, **26**, 1-11.

CHEN, C. T. and M. R. RODMAN (1985): Use of acid balance values to trace water-mass in the Weddell Sea. U. S. Antarctic Journal, 1985 Review, pp. 115–117.

CHEN, C. T. A. and M. R. RODMAN (1990): The inhomogeneous distribution of tritium and radiocarbon in the abyssal Southern Ocean. Terr. Atm. Ocean. Sci., **1** (1), 91–110.

CHIPMAN, D. W., T. TAKAHASHI and S. C. SUTHERLAND (1986): Carbon chemistry of the South Atlantic Ocean and the Weddell Sea: The results of the Atlantic Long Lines (AJAX) Expeditions, October, 1983 - February, 1984, Lamont-Doherty Geol. Obs., 185pp.

CHIPMAN, D. W. and T. TAKAHASHI (1990): Investigation of carbon chemistry in the Weddell Sea area during the 1986 winter expedition of the F/S Polarstern: June 28, 1986 - September 16, 1986, Lamont-Doherty Geol. Obs., 91pp.

CULBERSON, C. H., R. M. PYTKOWICZ and J. E. HAWLEY (1970): Seawater alkalinity determination by the pH method. J. Mar. Res. **28**, 15 –20.

DEACON, G. E. R. (1937): The hydrology of the Southern Ocean. Discovery Reports, **15**, 1–124.

DEACON, G. E. R. (1976): The cyclonic circulation in the Weddell Sea. Deep-Sea Res. **23**, 125–126.

DEACON, G. E. R. (1979): The Weddell Gyre. Deep –Sea Res. **26**, 981–995.

FOSTER, T. D. and J. H. MIDDLETON (1979): Variability in the bottom water of the Weddell Sea. Deep-Sea Res. **26A**, 743–762.

GEOSECS Atlantic Expedition (1981): Sections and Profiles, Vol. 2, A. E. Bainbridge, project director, National Science Foundation, Washington, D. C., 1–198.

GORDON, A. L. (1971): Antarctic Polar Front Zone. Antarctic Oceanology I. American Geophysical Union. Antarctic Research Series, **15**, 205–221.

GORDON, A. L. (1978): Deep Antarctic convection west of Maud Rise. J. Phys. Oceanogr. **8**, 600 –612.

GORDON, A. L. (1982): Weddell Deep Water variability. J. Mar. Res. **40**, suppl., 199–217.

GORDON, A. L., E. MOLINELLI and T. BAKER (1982): Southern Ocean Atlas. Columbia University Press, New York.

GORDON, A. L. and B. A. HUBER (1984): Thermohaline stratification below the Southern Ocean sea ice. J. Geophys, Res. **89**, 641–648.

GORDON, A. L., C. T. A. CHEN and W. G. METCALF (1984): Winter mixed layer entrainment of Weddell Deep Water. J. Geophys, Res., **89**, 637 –640.

HUBER, B. A., J. JENNINGS, C. T. CHEN, J. MARRA, S. RENNIE, P. MELE and A. GORDON (1983): Reports of the US–USSR Weddell Polynya Expedition: Vol. II Hydrographical data, LDGO 83–1, 218pp.

JACOBS, S. S. and D. T. GEORGI (1977): Obaervations on the Southwest Indian / Antarctic Ocean. *In*: A Voyage of Discovery, Ceorge Deacon 70th Anniversary Volume, M. ANGEL (ed.), Pergamon Press, Oxford, 43–84.

KILWORTH, P. D. (1979): On "chimney" formations in the ocean. J. Phys. Oceangr., **9**, 531–554.

KLEPIKOV, V. V. (1960): Warm deep waters in the Weddell Sea. Inform. Byul. Sov. Antark. Eksp., No. 17, 194–198.

KRYSELL, M. (1992): Carbon tetrachloride and methyl Chloroform as tracers of deep water formation in the Weddell Sea. Antarctica, Mar. Chem., **39**, 297–310.

LYNN, R. J. and J. L. REID (1968): Characteristics and circulation of deep and abyssal waters. Deep-Sea Res. **15**, 577–598.

MARTINSON, D. G., P. D. KILWORTH and A. L. GORDON (1981): A convective model for the Weddell Polynya. J. Phys. Oceanogr., **11**, 466 –488.

MONTGOMERY, R. B. (1958): Water characteristics of the Atlantic Ocean and of the World Ocean. Deep-Sea Res. **5**, 134–148.

ORSI, A. H., W. D. NOWLIN, Jr and T. WHITWORTH III (1993): On the circulation and stratification of the Weddell gyre. Deep-Sea Res., **40**, 169–203.

POISSON, A., and C. T. A. CHEN (1987): Why is there little anthropogenic CO_2 in the Antarctic Bottom Water? Deep-Sea Res., **34**, 1255–1275.

REID, J. L. and R. J. LYNN (1971): On the influence of the Norwegian-Greenland and Weddell Seas upon the bottom waters of the Indian and Pacific Oceans. Deep-Sea Res., **18**, 1063–1088.

REID, J. L., W. D. NOWLIN, Jr. and W. C. PATZERT (1977): On the characteristics and circulation of the southwestern Atlantic Ocean. J. Phys. Oceanogr., **7**, 62–91.

SCHLEMMER, F. C. (1978): Structure and spreading of Antarctic Bottom Waters in oceanic basins adjacent to Antarctica. Ph. D. dissertation, Texas A&M University, 127 pp.

WEISS, R. F., H. G. OSTLUND and H. CRAIG (1979): Geochemical studies of the Weddell Sea. Deep-Sea Res., **26**, 1093-1120.

WUST, G. (1939): The stratosphere of the Atlantic Ocean. The Scientific Results of the German Atlantic Expedition of the Research Vessel "Meteor" 1925-1927, Vol. VI, Section 1, W. J. EMERY (ed.), Amerind Publishing Co., New Delhi, 1-112.

ウエッデル海におけるpHの利用による水塊の追跡

Chen-Tung Arthur CHEN

要旨：東部ウエッデル海で得られたpHのデータを温位（θ）に対してプロットしたところ，θ＝0.08℃，σ_4＝46.06付近で明瞭な傾斜度の断絶が認められた。またθ＝−0.6℃，σ_4＝46.16付近でもこれよりやや不明瞭な断絶が生じた。全CO_2，pCO_2およびケイ酸のデータも同様な不連続性が見られた。このpH傾斜に見られる断絶は,おそらく深層および底層水塊に起因しているものと考えられ,両水塊の横方向への拡がりを識別する手助けとして利用できるものと考えられる。